International Journal of Chemical, Materials and Biomolecular Sciences
ISSN: 2415-6620
Vol:11, No:10, 2017

Towards the Integration of a Micro Pump in μTAS

Y. Haik

***Abstract*—**The objective of this study is to present a micro mechanical pump that was fabricated using SwIFT™ microfabrication surface micromachining process and to demonstrate the feasibility of integrating such micro pump into a micro analysis system. The micropump circulates the bio-sample and magnetic nanoparticles through different compartments to separate and purify the targeted bio-sample. This article reports the flow characteristics in the microchannels and in a crescent micro pump.

***Keywords*—**Crescent micropumps, microanalysis, nanoparticles.

I. Introduction

MICRO-MACHINED fluid components and systems, or microfluidics, have been one of the growth areas that lead to the forging of the MEMS term. Pioneered in the 1960s for fluid logic [1], microfluidic devices reemerged in the 1970s in the form of a miniature gas chromatograph and ink-jet printer nozzles [2]. Microfluidics research intensifies since 1990 due to the availability of fabrication processes and foundries. Our group has reported a number of microfluidic devices that are made out of silicon and polymers. We have produced a number of micropumps using the Sandia National Laboratory fabrication process. Our micropumps have been recognized for their integration of mechanical pumping principles in surface micromachining [3], [4]. Micro pumping principles have been a subject of investigation for last few decades. Pumping principles include the formation of bubbles by thermally heating the fluid to form bubbles that could either deform an adjacent membrane or push the fluid by the change of the bubble size [5]. However, the high temperature needed to boil fluids has limited this pumping principle. Charged fluids were separated by using a high voltage in an electro-osmotic pump [6]. Piezoelectric pumping utilizes the motion of a membrane that is subjected to an actuation force to induce the pumping of fluid [7].

The two general application areas of micropumps are those requiring precise metering of fluidic reagents and those where the pump needs to operate in a tightly confined space. Concrete examples of such application include implanted and transdermal drug delivery systems [8], micro Total Analysis Systems (μTAS) [9] and electronic cooling [10].

Unlike other fabrication technologies, surface micromachining of the mechanical micropumps ensures that all pumping and actuation components are made in the same process that reduces the challenges associated with ponding of a plurality of components. Surface micromachining provides a unique advantage over other fabrication technologies that it allows the simultaneous fabrication of pumping system along with the fluidic channels without extensive packaging. An external stimulus, such as a magnetic field for separation, could be introduced at the separation compartment without elaborating fabrication difficulties. Hence, the analysis system could be almost self-assembled during the fabrication process. The advantages of micro analysis devices include significant size, operation power, analyte consumption and fabrication reduction, enhancement of analytical performance, and precise control of fluid metering.

Magnetic nanoparticles with implanted surface affinity to targeted molecules are used to separate the targeted bio-molecule from the heterogeneous bio-sample. Upon mixing of the nanoparticles with bio-sample, the nanoparticles attach to the targeted bio-sample. Separation of targeted bodies is performed by an external magnetic field that attracts bio-sample loaded magnetic particles to a specific separation compartment.

In this study, the flow characteristics of nanofluids in microchannels made of silicon and polydimethylsiloxane-glass are reported. Microanalysis systems that utilize magnetic nanoparticles for separation of targeted species are sensitive, selective, reliable and require a low amount of the sample.

Silicon microchannels were fabricated at Sandia National Laboratories using a SwIFT™ microfabrication process. The channels had a height of 20 μm, width of 200 μm and length of 200 μm. Polydimethylsiloxane-glass (PDMS-glass) microchannels were fabricated at the Department of Chemistry, Florida State University with dimensions of 40 μm height, 200 μm width and 13 mm length.

Fluorescence correlation spectroscopy (FCS) was used to characterize the flow in both microchannels with 200 nm and 40 nm beads. It was found that the beads adsorb to the channels walls and agglomerate to prevent fluid motion. PDMS-glass microchannels had a maximum velocity equal to approximately 6.6 cm/s.

This study presents a micro mechanical pump that operates on the principle of positive displacement. The pump overcomes the challenges associated with conventional pumping principles.

II. Microfluidic Channels

SwIFT™ technology developed at Sandia National Laboratory was used to produce channels with an overall length of 500 μm, the straight portion of the channel is equal to 200 μm, the width is 20 μm and the height is approximately 6.8 μm (see Fig. 1). SwIFT™ utilizes silicon nitride instead of polysilicon to create transparent microfluidic channels [11]. The inlet and exit of these channels is introduced by a Bosch backside etch.

Y. Haik is with the Hamad Bin Khalifa University, Doha, Qatar (phone: +974 3045 3588; fax: +974 4454 0281; e-mail: yohaik@hbku.edu.qa).

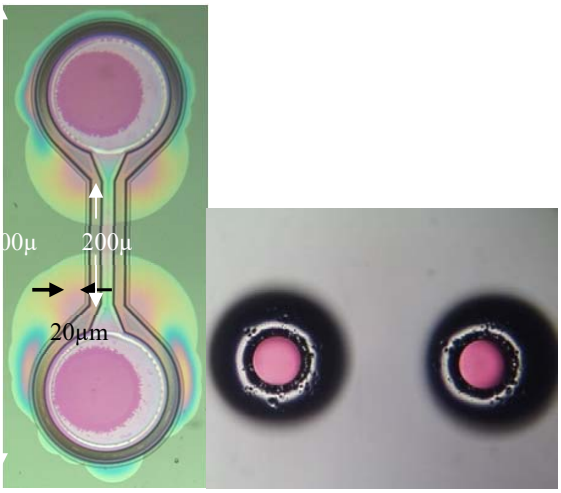

(a) Channel (b) Bosch etch in the backside

Fig. 1 Silicon micro channels fabricated by SwIFT™

III. Crescent Micro Pump

Crescent micropump was fabricated using Sandia National Laboratory's Sandia Ultra-planar, Multi-level, Micromachining Technology (SUMMiT V^{TM}). The pumping principle utilizes a ring gear driven through teeth on its outer surface to drive the pumping mechanism through teeth on its inner surface. The pump's inlet and exit are located inside the ring gear. Fig. 2 shows a photograph of the crescent pump. The pump is driven by a gear system that is motorized by an actuator attached to the gear system. The crescent pump has been utilized in many applications due to its reliability and reduced potential for leak. The pump operates with no valves and the fluid is contained in the vicinity of the ring gear making it naturally sealed from the outer devices.

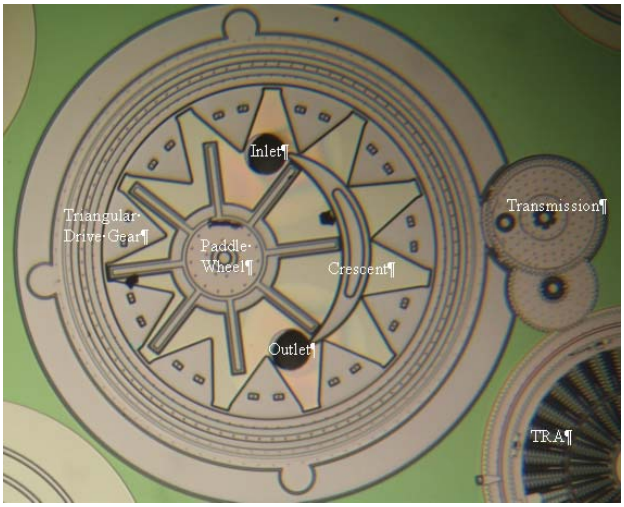

Fig. 2 Photograph of a crescent pump

The pumping principle of the crescent pump relies on the creation of partial vacuum that is generated by the out of mesh motion between the ring gear and the cut idler gear. The crescent divided the flow between the idler gear and the rotor. When the ring gear and the idler gear rotate, the gear teeth come out of mesh which draws the fluid into the pump. As the rotating gears mesh they increase the pressure near the outlet causing the fluid to pump out of the crescent pump.

The pump is driven by an external gear system that meshes with the outer gear perimeter of the crescent pump. The transmission gear system is connected to a TRA actuator.

The sealing approach used in the fabrication of the crescent pump employs pin joints to create a set of rollers, which act as axial bearings to support the walls of the seal during rotation and minimize friction. The mask layout employed in the implementation of the seal components are illustrated in Fig. 3. A structure defined in Poly1 and Poly2 and anchored to POLY0 provides sealing. Axial roller bearings defined in Poly2 and attached by pin joints to the ring support provide lateral support. On the right and left sides of the section Poly1 and Poly2 are laminated to form the external and internal teeth of the gear. On the left side of the section, a dimple cut is created on Poly1 to form a seal along the inside wall of the gear. Poly3 layer bridges the inner wall of the ring gear to the outer wall over the ring support. Dimple 3 cut is defined for the purpose of supporting the gear against the roller bearings. The section also shows two other dimple 3 cuts, which are smaller than the lateral support dimple 3. These two are created to provide vertical support while minimizing contact area between moving and stationary parts, thus minimizing contact area between moving and stationary parts, thus minimizing stiction and friction.

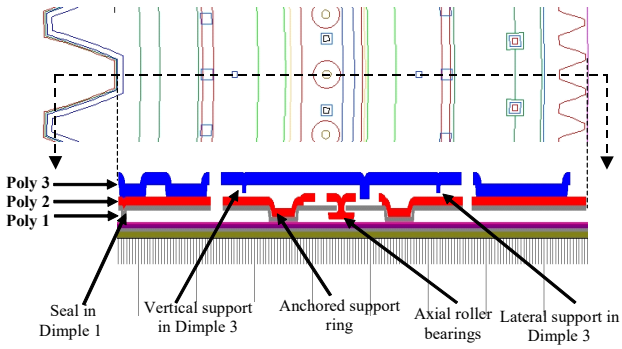

Fig. 3 A cross section through the ring gear of the offset planetary pump

IV. Pressure in Microchannels

The pressure drop in both the silicon and PDMS channels were investigated. A fluid reservoir with variable highest was used to feed the microchannels. The different elevations of the reservoir controlled the pressure head. The flow was monitored through the transparent tubes used to connect the reservoir to the microchannels. The pressure drop and velocity of the flow was measured for different elevations of the reservoir.

Fig. 4 shows the pressure versus Reynolds number when the fluid is water. The nonlinear behavior at high pressures is due to the change in the channel geometry due to the pressure

increase. The upper surface of the channel will bulge when subjected to high pressure. The Reynolds number showed that the flow is laminar.

Similar experiments were also conducted using PDMS channels. Fig. 5 shows the results obtained when the fluid used was water. The pressure relation showed a constant resistance.

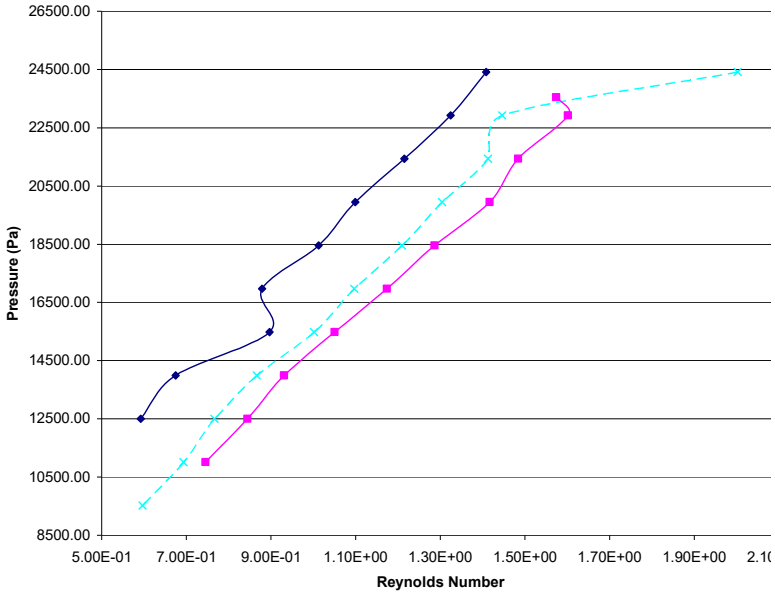

Fig. 4 Pressure Vs. Reynolds number-silicon channel

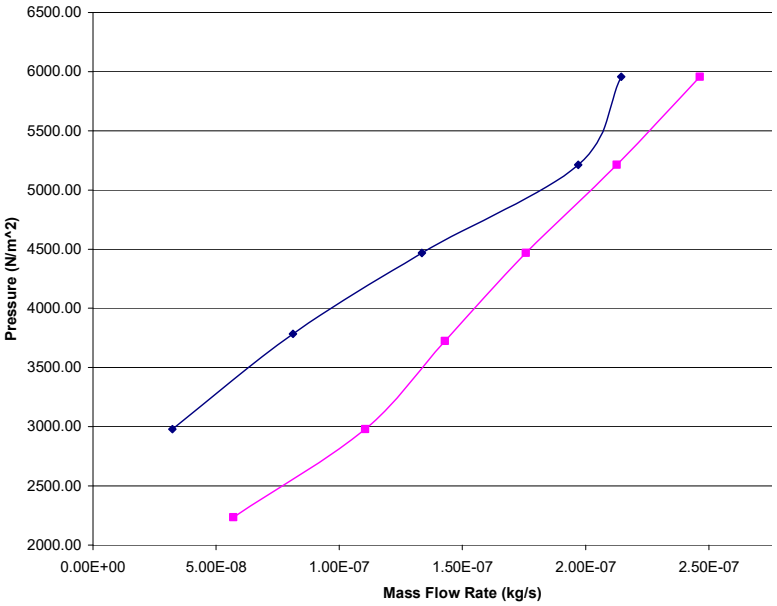

Fig 5 Pressure Vs Flow rate-PDMS Channel

V. Fluorescence Correlation Spectroscopy (FCS)

Fluorescent encapsulated nanoparticles were used to study the flow characteristic in the microchannels. FCS technique utilizes a laser (orange (540/560)) that excites fluorescent nanoparticles that travels through a predetermined confocal detection volume. The intensity of the fluorescence is recorded continuously and the travel time of a single particle through the predetermined volume of the laser can be extracted from the decay time of an autocorrelation curve [12].

Flow tests were performed in the silicon channel using florescent nanoparticles with diameter 40-200 nm (Molecular probes, FluoroSpheres®). The nanoparticles were prepared by diluting a 2% solid stock solution. The dilution was set to

50,000 times. The particles were then sonicated for 15 minutes before being introduced to the microchannels. The nanoparticles clogged the channel entrance and also agglomerated in the channel's wall. There are a number of reasons that could have caused the agglomeration; these include electrostatic attraction between the particles and the channel's wall, contamination of the fluid by bacteria that could cause adherence to of the fluorescent dye to the walls of the channel.

The area of agglomeration was investigated by scanning through the channel depth at steps of 1 µm increments. A scan, Fig. 6 (a), was done near the top nitride layer (~1 µm from upper surface) of the microchannel. Fig. 6 (b) shows the inside of the channel and shows that the beads in this area are agglomerated and appear to be stagnant.

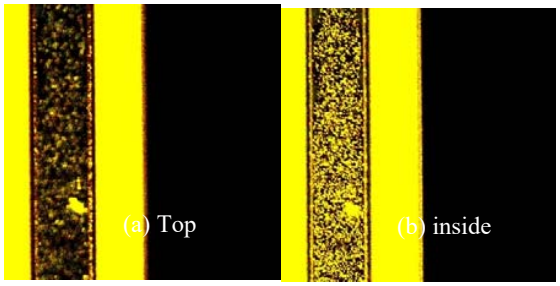

Fig. 6 Scan in the silicon channel

Velocity profile in PDMS-glass channels were investigated using FCS setup. The working solution for this experiment was a 70,000x dilution of the 40 nm FluoroSpheres® stock solution, 5% solid. Fig. 7 is a representation of the velocity profile across the channel. The near wall velocities could not be determined due to adsorption of the fluorescence beads to the wall. The max velocity point determined by FCS was 0.066 m/s.

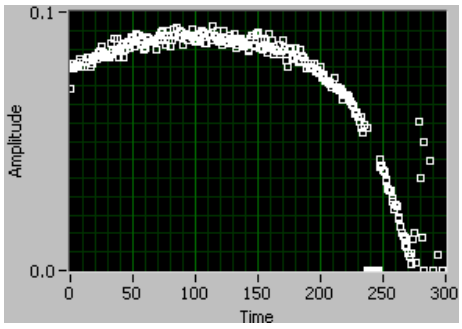

Fig. 7 Velocity profile in the PDMS channel

VI. Flow in Crescent Pump

The flow rate generated by a crescent pump could be expressed based on positive displacement of the fluid generated when the gears are rotating. The fluid is contained within two distinct volumes during its operation. The total volumetric flow rate can be described as:

$$\dot{Q} = \rho \cdot h(A_1 * n_1 * \omega_1 + A_2 * n_2 * \omega_2) \quad (1)$$

where Q is the mass flow rate, ρ is the density of the displaced fluid, h is the height of the pump, n_1 is the number of volumes on the paddle and n_2 is the number of triangular volumes on the triangular gear, $\omega_{1,2}$ are the frequencies at which the volumes are being moved and displaced.

At 8 Hz of the actuator operating frequency and pump's characteristics as shown in Table I, the flow rate can be determined for the crescent pump to be 5.04 x 10^{-10} kg/sec.

TABLE I
Flow Rate of Crescent Pump

Variable	Description	Value
ρ	Water density	997 kg/m^3
ω_1	ω 1	0.13 rad/sec at 8 Hz
ω_2	ω 2	0.17 rad/sec at 8 Hz
A_1	Area of gear 1	21,675 µm^2
A_2	Area of gear 2	13,080 µm^2
n_1	Number of teeth of gear 1	8
n_2	Number of teeth of gear 2	11
h	Distance between cover and pumping chamber floor	10.75 µm

The flow rate under the stated conditions is 5.04 x 10^{-10} kg/sec. To evaluate the theoretical flow rate, the pump was operated for different times. The actuator operated using a quarter sine wave signal at 40 volts and 8 Hz. The experimental data for the flow rates showed an average flow rate of 5.38 x 10^{-10} kg/sec at 8 Hz operational frequency of the TRA. The difference between the theoretical and experimental flow rate is 6%.

The pump flow rate at different frequencies without an applied pressure head is shown in Fig. 8. The result showed a linear increase between the flow rate and the operation angular speed which matches that of the theoretical equation.

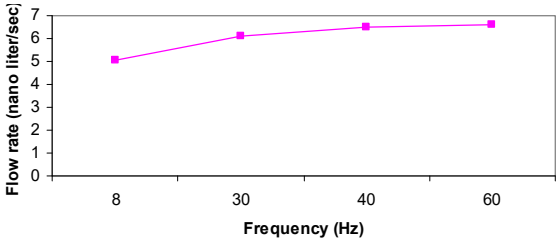

Fig. 8 Pump flow rate at different frequencies

VII. Conclusions

Flow characteristic in components of a microanalysis system are investigated. Flow in microchannels fabricated in silicon and PDMS-glass were reported. The pressure-flow rate in both channels showed a linear behavior. When nanospheres were introduced in the silicon channels they agglomerated and clogged the flow. However, in the PDMS channels the agglomeration was minimum. FCS showed a parabolic velocity profile in the micro channel. The flow in the crescent pump was investigated experimentally. The results showed an

agreement with the theoretical prediction.

ACKNOWLEDGMENT

The author acknowledges the contribution of Dr. M. Kilani, Mr. J. Hendrix and Mr. A. Zowelnski, who were students at Florida State University, where this work was conducted.

REFERENCES

[1] Kilani, M., Development of a Surface Micromachined Spiral-Channel Viscous Pump, The Florida State University, 2002
[2] Sosnowchik, B. D., Galambos, P. C., Sharp, K.V., Jenkins, M.W., Horn, M.W., Hendrix, J.R., SPIE, 2003
[3] Kilani M., Glambos P., Haik Y., Chen C-J. Design and Analysis of Surface Micromachined Spiral Channel Viscous Pump, Journal of Fluid Engineering, 152(2), 339-344, 2003.
[4] Chen C-J, Galambos P, Haik Y, Kilani M, Surface Micromachined Mechanical Micropumps and Fluid Shear Mixing, Lysing and Separation Microsystem, US Patent Application 20040126254, 2004.
[5] Tsai, Jr-Hung, Lin, Liwei, Journal of Microelectromechanical Systems, Vol. 11, NO. 6, 2002.
[6] Manz, A., Effenhauser, C.S., Burggraf, N., Harrison, D. J. Seller,, K., and Fluri, K., Journal of Micromechanics and Micro Engineering, Vol. 4, 1994.
[7] Moroney, R.M., White, R.M., and Howe, R.T, IEEE 1990 Ultrasonics Symposium Proceedings, Honolulu, 1990
[8] Hsu T-R. MEMS and Microsystems Design and Manufacture. New York, New York: McGraw-Hill, 2002.
[9] Blanchard R.J.W., Grotenhuis I., LaFave J.W., Perry Jr. J.F. Proceedings of the Society for Experimental Biology and Medicine 1965 Vol. 118; pages 465-468.
[10] Gupta P.K., Hung C. T. Journal of Encapsulation 1989; 427-462.
[11] Okandan Murat, (SPIE) Micromachining and Microfabrication Symposium; San Francisco, CA. SPIE Publishing; 2001. p. 133-39.
[12] Kalyan K. Kuricheti, Volker Buschmann, Paul Brister and Kennith D. Weston. Velocity Imaging in Microfluidic Devices using Fluorescence Correlation Spectroscopy. Department of Chemistry, The Florida State University.